NETWORK NEUROSCIENCE

an open access journal

Check for updates

Citation: Amico, E., & Goñi, J. (2018). Mapping hybrid functional-structural connectivity traits in the human connectome. *Network Neuroscience*, *2*(3), 306–322. https://doi.org/10.1162/netn_a_00049

DOI:
https://doi.org/10.1162/netn_a_00049

Supporting Information:
https://doi.org/10.1162/netn_a_00049
https://engineering.purdue.edu/CONNplexityLab

Received: 4 October 2017
Accepted: 14 February 2018

Competing Interests: The authors have declared that no competing interests exist.

Corresponding Author:
Joaquín Goñi
jgonicor@purdue.edu

Handling Editor:
Fabrizio De Vico Fallani

Copyright: © 2018
Massachusetts Institute of Technology
Published under a Creative Commons Attribution 4.0 International (CC BY 4.0) license

The MIT Press

FOCUS FEATURE:
Bridging Scales and Levels

Mapping hybrid functional-structural connectivity traits in the human connectome

Enrico Amico[1,2] **and Joaquín Goñi**[1,2,3]

[1]School of Industrial Engineering, Purdue University, West-Lafayette, IN, USA
[2]Purdue Institute for Integrative Neuroscience, Purdue University, West-Lafayette, IN, USA
[3]Weldon School of Biomedical Engineering, Purdue University, West-Lafayette, IN, USA

Keywords: Brain connectivity, Human connectome, Structural/functional patterns, Task-sensitive connectivity

ABSTRACT

One of the crucial questions in neuroscience is how a rich functional repertoire of brain states relates to its underlying structural organization. How to study the associations between these structural and functional layers is an open problem that involves novel conceptual ways of tackling this question. We here propose an extension of the Connectivity Independent Component Analysis (connICA) framework to identify joint structural-functional connectivity traits.

Here, we extend connICA to integrate structural and functional connectomes by merging them into common "hybrid" connectivity patterns that represent the connectivity fingerprint of a subject. We tested this extended approach on the 100 unrelated subjects from the Human Connectome Project. The method is able to extract main independent structural-functional connectivity patterns from the entire cohort that are sensitive to the realization of different tasks.

The hybrid connICA extracts two main task-sensitive hybrid traits. The first trait encompasses the within and between connections of dorsal attentional and visual areas, as well as frontoparietal circuits. The second trait mainly encompasses the connectivity between visual, attentional, default mode network (DMN), and subcortical network. Overall, these findings confirm the potential of the hybrid connICA for the compression of structural/functional connectomes into integrated patterns from a set of individual brain networks.

AUTHOR SUMMARY

A crucial question in neuroscience is how a rich functional repertoire of brain states relates to its underlying structural organization. How to study the associations between structural and functional layers is an open problem that requires novel conceptual frameworks. We here propose an extension of our connectivity independent component analysis (connICA) framework to integrate structural and functional connectomes and obtain hybrid connectivity fingerprints.

We use this method to extract two task-sensitive independent structural-functional connectivity patterns. The first encompasses the within and between connections of dorsal attentional and visual areas, as well as frontoparietal circuits. The second mainly encompasses the connectivity between visual, attentional, DMN, and subcortical networks.

Downloaded from http://www.mitpressjournals.org/doi/pdf/10.1162/netn_a_00049 by guest on 28 March 2024

These findings confirm the potential of hybrid connICA for the compression of structural/functional connectomes into integrated patterns.

INTRODUCTION

Brain connectomics is a rapidly growing area of research (Bullmore & Sporns, 2009; Fornito, Zalesky, & Bullmore, 2016). It is based on the investigation of functional and structural connections in the human brain, modeled as networks (Bullmore & Sporns, 2009; Fornito et al., 2016; Sporns, 2011). In large-scale brain network models, nodes correspond to gray matter regions (based on brain atlases or parcellations), whereas links or edges correspond to connections between the nodes. Structural connections are modeled from diffusion-weighted imaging (DWI) data by inferring the main white matter axonal pathways between brain region pairs through tractography algorithms (Fornito et al., 2016), normally denominated by structural connectome or connectivity (SC; Sporns, 2011). Functional connections are modeled from functional magnetic resonance imaging (fMRI) data by measuring temporal statistical dependences between the estimated neural activity of brain region pairs while subjects are either at rest or performing a task in the scanner, usually defined as functional connectivity of connectome (FC; Fox & Raichle, 2007; Friston, 2011).

Network:
an ordered pair formed by a set of nodes and a set of edges (which represent connections between pairs of nodes). Nodes are usually represented by circles, whereas edges are represented by lines or arcs connecting pairs of nodes.

Diffusion-weighted imaging (DWI):
a magnetic resonance imaging (MRI) technique based on measuring the random Brownian motion of water molecules within a voxel based on sampling 3D directions. This technique allows for estimating white matter streamlines and fiber bundles connecting brain regions.

Tractography:
computational reconstruction procedure that may be used to obtain, from DWI data, white matter streamlines or fiber tracts connecting different brain regions.

Connectome or structural connectivity (SC) matrix:
a network representation of the physical connections in the brain. Nodes represent brain regions, whereas edges represent physical connections of pairs of brain regions through the white matter. Weights typically denote the density or also the integrity of the connections.

Functional magnetic resonance imaging (fMRI):
a noninvasive technique that estimates brain activity by detecting changes associated with blood flow. The rationale of this technique relies on the fact that there is a positive association between cerebral blood flow and neuronal activation.

The exponential growing of publicly available neuroimaging datasets in recent years has allowed researchers to make inferences on the different organization of brain networks in clinical and healthy populations, and to identify changes in these cohorts (Fornito, Zalesky, & Breakspear, 2015; Fornito et al., 2016), both at the structural and functional level. During the past few years, many efforts have also been made to address one of the crucial questions in brain connectomics. That is, how a rich functional repertoire of brain states relates to its underlying structural organization, especially at the large scale of cortical/subcortical gray matter modules and white matter fiber bundles (Falcon, Jirsa, & Solodkin, 2016; Goñi et al., 2014; Honey et al., 2009; Honey, Kötter, Breakspear, & Sporns, 2007; Honey, Thivierge, & Sporns, 2010).

The study of the associations between these structural and functional layers (Mišić et al., 2016) is difficult to accomplish because of several factors. One factor is related to obtaining individual accurate connectivity patterns. This involves the following: the design of MRI sequences for structural imaging, DWI, and fMRI; the development of processing pipelines to process MRI data; and a brain parcellation or atlas to reduce the dimensionality from gray matter voxels to brain regions and criteria to estimate levels of structural and functional coupling.

Another aspect relates to the intersubject variability of these two modalities. The identification of group-level structure-function relationships (Mišić et al., 2016) may become an even more powerful approach if individual estimations were taken into account. As a matter of fact, it has recently been shown that the "individual fingerprint" of a functional connectome (Finn et al., 2015) is a key property for investigating further inferences and links between connectomics and genetic, demographic, or clinical variables (Shen et al., 2017). The recent trend goes, therefore, toward working at the single-subject level and toward the refinement and improvement of this individual signature in an individual human connectome (Amico & Goñi, 2017). In this sense, providing not only group-level SC or covarying SC/FC patterns but also their individual estimations is an important step forward. Lastly, the vast amount of information contained in both functional and structural connectomes is problematic for the investigation of joint FC and SC patterns. In this scenario, the researcher has to extract

Downloaded from http://www.mitpressjournals.org/doi/pdf/10.1162/netn_a_00049 by guest on 28 March 2024

Functional connectome/connectivity (FC) matrix:
a network representation of the functional coupling between brain regions. Such coupling is usually measured by quantifying the statistical dependencies between time series of brain regions (e.g., pairwise Pearson's correlation, mutual information) as obtained by functional magnetic resonance imaging (fMRI).

Independent component analysis (ICA):
a computational method for disentangling the independent additive subcomponents of a multivariate input signal, under the assumption that the subcomponents are non-Gaussian signals and that they are statistically independent from each other.

and compress informative features from hundreds of functional and structural connectomes separately, from either healthy or clinical populations, and then come up with creative ways to merge the extracted functional information with its structural counterpart, or find ways to compress them in some integrative framework.

We here define an extension of our recently proposed connectivity-based independent component analysis (i.e., connICA; Amico et al., 2017) technique, to overcome the aforementioned issues. The connICA methodology implements independent component analysis (ICA) for the extraction of robust independent functional connectivity patterns from a set of individual functional connectomes, without imposing any a priori data stratification into groups (Amico et al., 2017). Here, we extend connICA to include both structural and functional connectomes by merging them into a common "hybrid" matrix (see scheme in Figure 1) that includes both the structural and functional fingerprint of each subject (Amico & Goñi, 2018). We tested this extended approach on the 100 unrelated subjects taken from the Human Connectome Project (details on the project available at http://www.humanconnectome.org/) and evaluated it for two brain parcellations. We here show how this method is able to extract main independent structure-function couplings with individual estimations for the entire population of subjects, and to disentangle the joint functional-structural subsystems that are sensitive to different functional tasks (including also resting state).

These findings confirm the potential of the hybrid connICA for the compression of meaningful information out of a set of heterogeneous brain networks based on both functional and structural connectomes while capturing individual differences. We conclude by discussing limitations and potential future directions for this methodology.

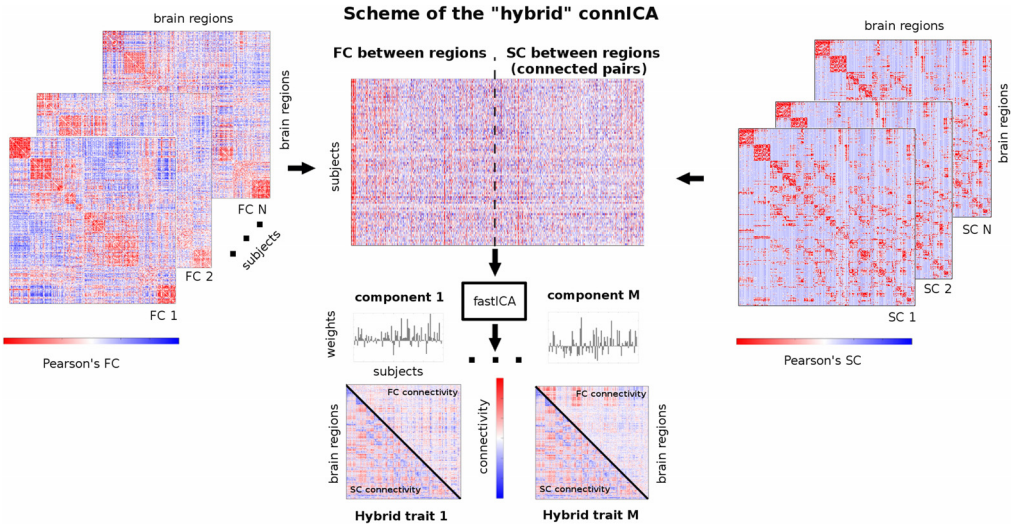


Figure 1. Workflow scheme of the hybrid connICA. The upper triangular of each individual functional connectivity (FC) matrix (left) and lower triangular of each correspondent structural connectivity profile (SC) are added to a matrix where rows are the subjects and columns are their vectorized hybrid (structural-functional) connectivity patterns. Note that for SC, only connected pairs across all subjects were included (see Materials and Methods section for details). The ICA algorithm extracts the M independent components (i.e., hybrid traits) associated to the whole population and their relative weights across subjects. Colorbars indicate positive (red) and negative (blue) connectivity values: Pearson's correlation coefficient values in the case of individual FC and SC matrices (left and right side of scheme), and unitless connectivity weights in the case of hybrid traits (bottom of the scheme).

Downloaded from http://www.mitpressjournals.org/doi/pdf/10.1162/netn_a_00049 by guest on 28 March 2024

MATERIALS AND METHODS

Dataset

The functional and structural dataset used in this work is from the Human Connectome Project (HCP; http://www.humanconnectome.org/), Release Q3. Per HCP protocol, all subjects gave written, informed consent to the Human Connectome Project consortium. Below is the full description of the acquisition protocol and processing steps.

HCP: Functional Data

We used fMRI runs from the 100 unrelated subjects of the HCP 900 subjects data release (Van Essen et al., 2012; Van Essen et al., 2013). The fMRI resting-state runs (HCP filenames: rfMRI_REST1 and rfMRI_REST2) were acquired in separate sessions on two different days, with two different acquisitions (left to right, or LR, and right to left, or RL) per day (Glasser et al., 2013; Van Essen et al., 2012; Van Essen et al., 2013). The seven fMRI tasks were the following: gambling (tfMRI_GAMBLING), relational (tfMRI_RELATIONAL), social (tfMRI_SOCIAL), working memory (tfMRI_WM), motor (tfMRI_MOTOR), language (tfMRI_LANGUAGE, including both a story-listening and arithmetic task), and emotion (tfMRI_EMOTION). The working memory, gambling, and motor task were acquired on the first day, and the other tasks were acquired on the second day (Barch et al., 2013; Glasser et al., 2013). The HCP scanning protocol was approved by the local Institutional Review Board at Washington University in St. Louis. For all sessions, data from both the LR and RL phase-encoding runs were used to calculate connectivity matrices. Full details on the HCP dataset have been published previously (Barch et al., 2013; Glasser et al., 2013; S. M. Smith et al., 2013).

HCP: Structural Data

We used DWI data from the same 100 unrelated subjects of the HCP 900 subjects data release (Van Essen et al., 2012; Van Essen et al., 2013). The diffusion acquisition protocol is covered in detail elsewhere (Glasser et al., 2013; Sotiropoulos et al., 2013; Uğurbil et al., 2013). Below we mention the main characteristics. Very high resolution acquisitions (1.25 mm isotropic) were obtained by using a Stejskal-Tanner (monopolar) (Stejskal & Tanner, 1965) diffusion-encoding scheme. Sampling in q-space was performed by including three shells at b = 1,000, 2,000 and 3,000 s/mm^2. For each shell corresponding to 90 diffusion gradient directions and 5 b = 0's acquired twice were obtained, with the phase-encoding direction reversed for each pair (i.e., LR and RL pairs). Directions were optimized within and across shells (i.e., staggered) to maximize angular coverage by using the approach of Caruyer et al. (2011; http://www-sop.inria.fr/members/Emmanuel.Caruyer/q-space-sampling.php) and to form a total of 270 noncollinear directions for each phase-encoding direction. Correction for EPI and eddy current–induced distortions in the diffusion data was based on manipulation of the acquisitions so that a given distortion manifested itself differently in different images (Andersson, Skare, & Ashburner, 2003). To ensure better correspondence between the phase-encoding reversed pairs, the whole set of diffusion-weighted (DW) volumes was acquired in six separate series. These series were grouped into three pairs, and within each pair the two series contained the same DW directions but with reversed phase encoding (i.e., a series of Mi DW volumes with RL phase encoding is followed by a series of Mi volumes with LR phase encoding, i = [1,2,3]).

Brain Atlases

We employed a cortical parcellation into 360 brain regions as recently proposed by Glasser et al. (2016). For completeness, 14 subcortical regions were added, as provided by the HCP

Downloaded from http://www.mitpressjournals.org/doi/pdf/10.1162/netn_a_00049 by guest on 28 March 2024

release (filename "Atlas_ROI2.nii.gz"). To do so, this file was converted from NIFTI to CIFTI format by using the HCP workbench software (Glasser et al., 2013; Marcus et al., 2011) (command *-cifti-create-label*; http://www.humanconnectome.org/software/connectome-workbench.html). An additional parcellation scheme was also evaluated (Destrieux, 164 brain regions; Destrieux, Fischl, Dale, & Halgren, 2010; Fischl et al., 2004; as available in FreeSurfer).

HCP Preprocessing: Functional Data

The HCP functional preprocessing pipeline (Glasser et al., 2013; S. M. Smith et al., 2013) was used for the employed dataset. This pipeline included artefact removal, motion correction, and registration to standard space. Full details on the pipeline can be found in Glasser et al. (2013) and S. M. Smith et al. (2013). The main steps were the following: spatial ("minimal") preprocessing, in both volumetric and grayordinate forms (i.e., where brain locations are stored as surface vertices; S. M. Smith et al., 2013); weak high-pass temporal filtering (>2,000 s full width at half maximum) applied to both forms, achieving slow drift removal; MELODIC ICA (Jenkinson, Beckmann, Behrens, Woolrich, & Smith, 2012) applied to volumetric data; artifact components identified using FIX (Salimi-Khorshidi et al., 2014). Artifacts and motion-related time courses were regressed out (i.e., the 6 rigid-body parameter time series, their backward-looking temporal derivatives, plus all 12 resulting regressors squared) of both volumetric and grayordinate data (S. M. Smith et al., 2013).

For the resting-state fMRI data, we also added the following steps: global gray matter signal was regressed out of the voxel time courses (Power et al., 2014); a band-pass first-order Butterworth filter in forward and reverse directions [0.001 Hz, 0.08 Hz] (Power et al., 2014) was applied (Matlab functions *butter* and *filtfilt*); the voxel time courses were z scored and then averaged per brain region, excluding outlier time points outside of 3 standard deviation from the mean, using the workbench software (Marcus et al., 2011) (workbench command *-cifti-parcellate*). For task fMRI data, we applied the same above mentioned steps, with a less restrictive range for the band-pass filter [0.001 Hz, 0.25 Hz].

Pearson correlation coefficients between pairs of nodal time courses were calculated (MATLAB command *corr*), resulting in a symmetric connectivity matrix for each fMRI session of each subject. Functional connectivity matrices from the LR and RL phase-encoding runs were averaged to improve signal-to-noise ratio. The functional connectomes were kept in their signed weighted form, hence neither thresholded nor binarized. This was done for the two parcellations described above, namely Glasser with subcortical regions added (giving a total of 374 brain regions) and Destrieux (164 brain regions).

Finally, the resulting individual functional connectivity matrices were ordered (rows and columns) according to seven resting-state cortical subnetworks (RSNs) as proposed by Yeo et al. (2011). For completeness, an eighth subnetwork including the 14 HCP subcortical regions was added (as analogously done in a recent paper; Amico et al., 2017).

HCP Preprocessing: Structural Data

The HCP DWI data were processed following the MRtrix3 (Tournier, Calamante, & Connelly, 2012) guidelines (http://mrtrix.readthedocs.io/en/latest/tutorials/hcp_connectome.html). In summary, we first generated a tissue-segmented image appropriate for anatomically constrained tractography (ACT; R. E. Smith, Tournier, Calamante, & Connelly, 2012; MRtrix command *5ttgen*); we then estimated the multishell multitissue response function (Christiaens et al., 2015), MRtrix command *dwi2response msmt_5tt*) and performed the multishell, multitissue

Downloaded from http://www.mitpressjournals.org/doi/pdf/10.1162/netn_a_00049 by guest on 28 March 2024

constrained spherical deconvolution (Jeurissen, Tournier, Dhollander, Connelly, & Sijbers, 2014; MRtrix *dwi2fod msmt_csd*); afterward, we generated the initial tractogram (MRtrix command *tckgen*, 10 million streamlines, maximum tract length = 250, FA cutoff = 0.06) and applied the successor of spherical-deconvolution informed filtering of tractograms (SIFT2; R. E. Smith, Tournier, Calamante, & Connelly, 2015) methodology (MRtrix command *tcksift2*). Both SIFT (R. E. Smith, Tournier, Calamante, & Connelly, 2013) and SIFT2 (R. E. Smith et al., 2015, p. 2) methods provide more biologically meaningful estimates of structural connection density. SIFT2 allows for a more logically direct and computationally efficient solution to the streamlines connectivity quantification problem: by determining an appropriate cross-sectional area multiplier for each streamline rather than removing streamlines altogether, biologically accurate measures of fiber connectivity are obtained while making use of the complete streamlines reconstruction (R. E. Smith et al., 2015). Then, we mapped the SIFT2 outputted streamlines onto the 374 chosen brain regions (360 from Glasser et al., 2016, brain atlas plus 14 subcortical regions; see Brain Atlases section) to produce a structural connectome (MRtrix command *tck2connectome*). Finally, a $\log_{10}$ transformation (Fornito et al., 2016) was applied on the structural connectomes to better account for differences at different magnitudes. Consequently, SC values ranged between 0 and 5 on this dataset. To test the method with a different parcellation scheme, we performed the same mapping steps from the streamlines to a second parcellation (Destrieux, 164 brain regions; Destrieux et al., 2010; Fischl et al., 2004; as available in FreeSurfer).

Hybrid connICA: Independent Component Analysis of Joint Functional and Structural Connectomes

The potential of multidimensional feature extraction from different neuroimaging modalities has been already introduced and explored (Calhoun et al., 2006a, 2006b; Calhoun, Liu, & Adali, 2009) in the fMRI domain. Recently, applications of ICA (Hyvärinen & Oja, 2000) in the functional connectome domain (Amico et al., 2017; Kessler, Angstadt, & Sripada, 2016) and in joint patterns of functional connectomes and gray/white matter volumes (Kessler, Angstadt, Welsh, & Sripada, 2014) have been investigated. Here we propose a framework that allows for the extraction of joint connectivity traits from a set of functional and structural connectomes based on the extension of our recently proposed connICA (Amico et al., 2017), here named "hybrid connICA." Below is the detailed description of the hybrid connICA scheme.

The first step relates to uniforming the different distributions of FC values (Pearson's correlation values ranging between -1 and 1) and SC values (after $\log_{10}$ transformation, ranging between 0 and 5). There are several options to normalize FC and SC connections in the same range: here we proceeded as follows. For each pair of nodes i and j directly connected in the SC matrix, we evaluated their "structural correlation," that is, the Pearson's correlation coefficient between the i_{th} and j_{th} row of the structural connectome. Iterating this procedure over all connected pairs gives a correlation matrix of a structural connectome (see Figure S2 of the Supplemental Material, Amico & Goñi, 2018). The values in this matrix range between between -1 and 1, with negative values indicating two nodes that are connected antagonistically to the rest of the network, and positive indicating high similarity in their structural connections with the rest of the brain network. This solution, similarly to matching index (Rubinov & Sporns, 2010), provides several advantages: it does not change the general properties of the SC (Figure S2) and it also allows to have functional and structural connectomes in the same range between -1 and 1. However, this transformation also changes the SC matrix structure from sparse to full. Therefore, in order for this correlation matrix to be representative of the real structural architecture of a human brain, we only considered the correlation values corresponding to structurally connected pairs of brain regions (i.e., edges with nonzero values

Downloaded from http://www.mitpressjournals.org/doi/pdf/10.1162/netn_a_00049 by guest on 28 March 2024

in all the SCs of the population; this corresponds to approximately 21% of all possible pairs; see Figure S2).

The second step is similar to the standard connICA approach (Amico et al., 2017): the input of the hybrid connICA consists of all the individual FC and SC profiles embedded into a "hybrid" dataset matrix where each row contains all the edges of the upper triangular part of an individual FC matrix (first half) and the correspondent lower triangular part of the SC matrix from the same individual (second half; see scheme at Figure 1). Note that due to symmetry of Pearson's correlations on FC and SC, taking the upper or the lower part of both matrices is just conventional. In this cross-sectional study, we selected 10 different subjects per task (7 tasks and 1 resting state; see HCP: Functional Data section), ending up with a hybrid matrix of 80 hybrid connectivity profiles. Each profile represents the unique hybrid connectivity signature (both structural and functional) of a human brain (Figure 1). Note that this method is insensitive to the ordering of the columns on the input hybrid matrix (i.e., it does not affect the results obtained).

Principal component analysis (PCA): a statistical procedure that uses an orthogonal transformation to convert a set of observations of possibly correlated variables into a set of values of linearly uncorrelated variables called principal components.

Before running the ICA algorithm, dimensionality reduction on the dataset was obtained by applying principal component analysis (PCA; Jolliffe, 2014) on the hybrid matrix. The advantage of applying PCA before ICA for noise filtering and dimensionality reduction in order to avoid overfitting has already been shown, both by the machine learning (Särelä & Vigário, 2003) and neuroimaging communities (Calhoun et al., 2006a; Kessler et al., 2014). Recently, we also showed that PCA decomposition and subsequent reconstruction of functional connectomes can increase individual identifiability in a population by retaining an optimal number of principal components (which usually explained the 90% of the variance in the functional data employed; see Amico & Goñi, 2017). Here, we applied PCA to compress and reduce the dimensionality of the data by keeping the principal components explaining 90% of the variance of the initial hybrid data. Indeed, since the hybrid input matrix is highly redundant (due to high similarity in structural healthy connectomes, as well as task-based FCs), 40 components explained 90% of variance in the data (see Figure S1 of the Supplemental Material, Amico & Goñi, 2018).

Next, ICA decomposition of the PCA-reconstructed hybrid matrix was applied by running the FastICA algorithm (Hyvarinen, 1999). Similarly to connICA (Amico et al., 2017), the output of the hybrid connICA consists of two vectors per component. The first output vector will be referred to as hybrid trait, which represents an independent pattern of joint functional-structural connectivity, common to the whole population. The second output vector is the weight of the hybrid trait on each subject, which quantifies the prominence or presence of the trait in each individual connectivity hybrid profile (both functional and structural). This methodology allows for compressing the information contained in a population of structural and functional connectomes into a few connectivity traits and unique individual weights associated to them. This can greatly ease the process of making inferences between the hybrid connectivity subsystems present in a single-subject structural-FC profile and genetic, demographic, or clinical variables at hand.

Given the nondeterministic nature of the FastICA decomposition into components (Hyvarinen, 1999), it is very important to run it several times and only select the most robust outcomes, in this case hybrid traits. We evaluated the robustness of the traits over 100 FastICA runs, as in (Amico et al., 2017). A bootstrap technique was used to accurately estimate the hybrid traits from the 100 subjects pool of the HCP dataset (see Hybrid connICA: Independent Component Analysis of Joint Functional and Structural Connectomes section for details). At

Downloaded from http://www.mitpressjournals.org/doi/pdf/10.1162/netn_a_00049 by guest on 28 March 2024

every run, random samples comprising hybrid profiles from 80 different subjects (10 subjects per task and resting state) were performed. This was meant to avoid results driven by a small subset of the population. Finally, a hybrid trait was considered robust when it appeared (correlation of 0.5 or higher across runs) in at least 50% of the runs and its representation consisted of the average across all its appearances over the 100 runs.

The last point worth mentioning about the procedure relates to the number of independent components chosen. There is not a gold standard for this choice: it usually depends on heuristic measures and the dataset at hand (Calhoun et al., 2009; Hyvärinen & Oja, 2000). Since here the main aim of the study was to investigate joint FC-SC task-dependent hybrid traits, we assessed the number of ICA components (ranging from 2 up to the dimension of the hybrid matrix after PCA reconstruction; see Figure S1) that would maximize both the number of robust hybrid traits and task-based intraclass correlation (ICC) on their weights (see next section for details). This heuristic measure resulted in an optimal choice of 10 independent components (see Figure S1).

Intraclass correlation (ICC): an inferential statistic for quantitative measurements that are organized into groups. It describes how strongly units in the same group resemble each other. A typical application consists of the assessment of consistency or reproducibility of quantitative measurements made by different observers measuring the same quantity.

Task-Based Sensitivity

We quantified whether a hybrid trait was task sensitive by using intraclass correlation (Bartko, 1966; Shrout & Fleiss, 1979). ICC is a widely used measure in statistics, normally to assess the percent of agreement between units (or ratings/scores) of different groups (or raters/judges) (McGraw & Wong, 1996). It describes how strongly units in the same group resemble each other. The stronger the agreement, the higher its ICC value. We used ICC to quantify to what extent the individual values of the weights of an hybrid trait could separate between subjects performing different tasks. Following this rationale, the different tasks are "raters" and "scorers" given by the individual hybrid weights of the subjects. In this case, the higher the ICC, the more separable the different tasks across subjects and consequently the more task dependent (i.e., higher changes in the weights) in the correspondent hybrid traits.

Structural Connectome Randomization

To avoid the possibility that the hybrid patterns were only driven by the functional profiles, we ran the hybrid connICA with randomized structural connectomes. The edges of each individual SC were swapped 50,000 times, following the randomization technique proposed in (Goñi, Corominas-Murtra, Solé, & Rodríguez-Caso, 2010). This randomization preserves the main topological properties of the structural connectomes, such as size, density and degree sequence (and hence degree distribution; Goñi et al., 2010). The chosen number of swaps (50,000) represents the best trade-off for this data between minimum number of swaps and maximum gain in dissimilarity of the randomized connectomes with respect to the original SCs (see Figure S2).

RESULTS

The dataset used for this study consisted of structural and functional data from the 100 unrelated subjects in the Q3 release of the HCP (Van Essen et al., 2012, 2013). For each subject, we estimated eight functional connectivity matrices, one corresponding to resting state (by averaging the REST1_LR and REST1_RL FCs), seven corresponding to each of the seven tasks (by averaging LR and RL corresponding FCs; see Materials and Methods); and one structural connectome, corresponding to the HCP DWI acquisition S1 (see Materials and Methods). The multimodal parcellation used here, as proposed by Glasser et al. (2016), includes 360 cortical

Downloaded from http://www.mitpressjournals.org/doi/pdf/10.1162/netn_a_00049 by guest on 28 March 2024

brain regions. We added 14 subcortical regions, hence producing functional connectome matrices (square, symmetric) of 374 × 374 (see Materials and Methods for details).

From the test-retest pool of 100 unrelated subjects (total of 800 FC matrices and 100 SC matrices), a bootstrap technique was used to accurately estimate the task-dependent hybrid traits. That is, for each run of hybrid connICA, a random cross-sectional sample comprising the functional-structural connectomes pairs of 80 subjects (10 subjects per task and resting state) was considered. This was meant to avoid results driven by a small subset of the population and to minimize redundancy in the SCs due to including the same subjects performing different tasks.

The hybrid connICA procedure can be summarized as follows (Figure 1; see also Amico et al., 2017): First, the upper and lower triangular parts of each individual FC and SC were vectorized and added to a matrix where rows are the subjects and columns are their full connectivity pattern; second, the ICA algorithm was run (100 runs, number of IC = 10; see Materials and Methods) to extract the main hybrid (joint FC-SC) traits associated to the whole population; and third, the most robust (appearing at least 50% of the times with correlation higher than 0.5; see Materials and Methods) and task-dependent components (as measured by intraclass correlation on the weights per different task/resting session; see Materials and Methods) were selected.

The hybrid connICA procedure resulted in two main task-sensitive hybrid traits (Figure 2). The frequency of the averaged hybrid traits across runs were 90% and 89% respectively. That is, the main functional-structural patterns, common to the whole population, which weights change depending on the task that is being performed (high values of task-based intraclass correlation: 0.65 and 0.70; see Figure 2A1 and 2A2). A third robust averaged hybrid trait (64% frequency across runs) was obtained through hybrid connICA (Figure S4), which, however, was not task sensitive (ICC = 0.16). Interestingly, this trait encompasses the main resting-state networks and corresponding within-network structural connections (Figure S4).

Among the task-dependent hybrid traits, the functional part of the first trait mainly captures the within-connectivity of dorsal and visual networks, as well as interconnections among dorsal attentional, visual, and subcortical networks (Figure 2). The structural part mainly evidences the within-network connectivity between these aforementioned three networks. The functional part of the second trait mainly represents the connectivity between the visual, attentional (dorsal and ventral), DMN, frontoparietal (FP), and subcortical networks (Figure 2). The structural part mainly captures the within-network connectivity between those and the limbic system. It is worth mentioning here one of the advantages of the hybrid connICA procedure: The hybrid traits represent joint structural-functional profiles learned from the whole population at the same time (the subject weights corresponding to the FC or SC are the same).

To assess the generalization of these results with respect to the gray matter parcellation used, we ran the same analyses with a lower resolution parcellation, namely Destrieux atlas (Destrieux et al., 2010; Fischl et al., 2004; as available in FreeSurfer software) which includes 164 brain regions. The two most frequent averaged hybrid traits (92% and 97%, respectively) are shown in Figure S5. Both hybrid traits were task sensitive (ICC being 0.60 and 0.58, respectively). When comparing the hybrid traits obtained from both parcellations (Figure 2 and Figure S5), we observed a high resemblance from the perspective of an RSN (within and between).

Downloaded from http://www.mitpressjournals.org/doi/pdf/10.1162/netn_a_00049 by guest on 28 March 2024

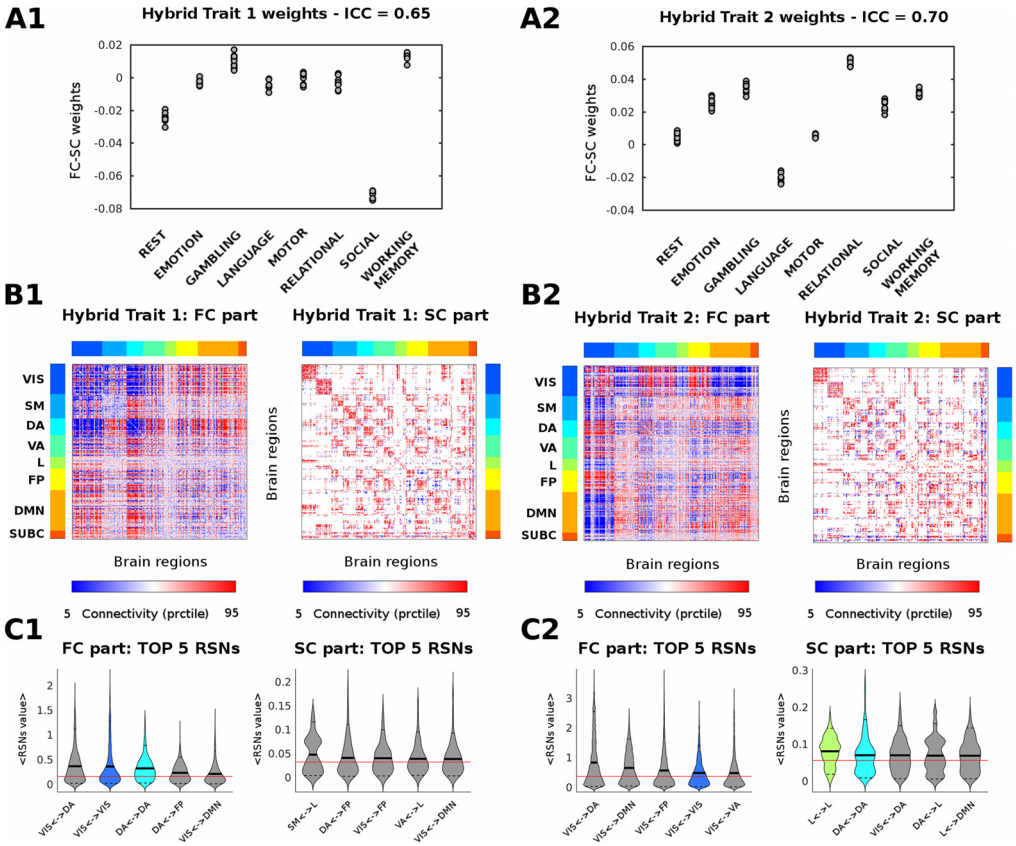


Figure 2. Mapping of the main task-sensitive hybrid traits. (A1 and A2) Quantified presence of each hybrid trait on each individual functional connectome. Subject weights are grouped according to each of the seven tasks and resting state (10 subjects per task and resting state; see Materials and Methods). Task-based intraclass correlation values are reported on top. (B1 and B2) Visualization of the two hybrid traits associated to significant changes (as measured by ICC) between tasks and resting state. For ease of visualization, the hybrid traits are split in two matrices, corresponding to the functional connectivity (FC) and structural connectivity (SC) patterns. The brain regions are ordered according to functional RSNs (Yeo et al., 2011): visual (VIS), somatomotor (SM), dorsal attention (DA), ventral attention (VA), limbic system (L), frontoparietal (FP), default mode network (DMN), and for completeness, also subcortical regions (SUBC). (C1 and C2) Violin plot of hybrid trait values for the top five RSNs. The top five edge distributions per within or between RSNs interaction are shown separately for the FC and SC profiles. Each color indicates a different within-RSN (as in B and C RSN colorbars), whereas gray indicates edge values between RSN networks. The solid black lines of the violins depict the mean value of the distribution; the dashed black lines the 5 and 95 percentiles; the solid red line indicates the whole-brain mean value.

We then mapped each resulting hybrid connectivity profile onto a brain cortical surface (Figure 3). First we created a "hybrid mask" by taking only the most extreme edges in the FC and SC parts of the two hybrid traits (outside the 5th and 95th percentile of each distribution of values; see Figure 3). That binary mask was then mapped onto a brain cortical mesh to visualize the main hybrid circuitry involved in task switching (Figure 3). This allows to examine simultaneously functional nodes and structural pathways that are sensitive (i.e., differently engaged) along the tasks. In the case of the first trait, the dorsal cortical regions are more prominent, as expected, as are their interhemispheric structural connections, as well as the fibers projecting from these regions to subcortices and frontal areas (Figure 3). For the second trait, visual cortices are the most prominent functionally, as well as the pathways connecting

Downloaded from http://www.mitpressjournals.org/doi/pdf/10.1162/netn_a_00049 by guest on 28 March 2024

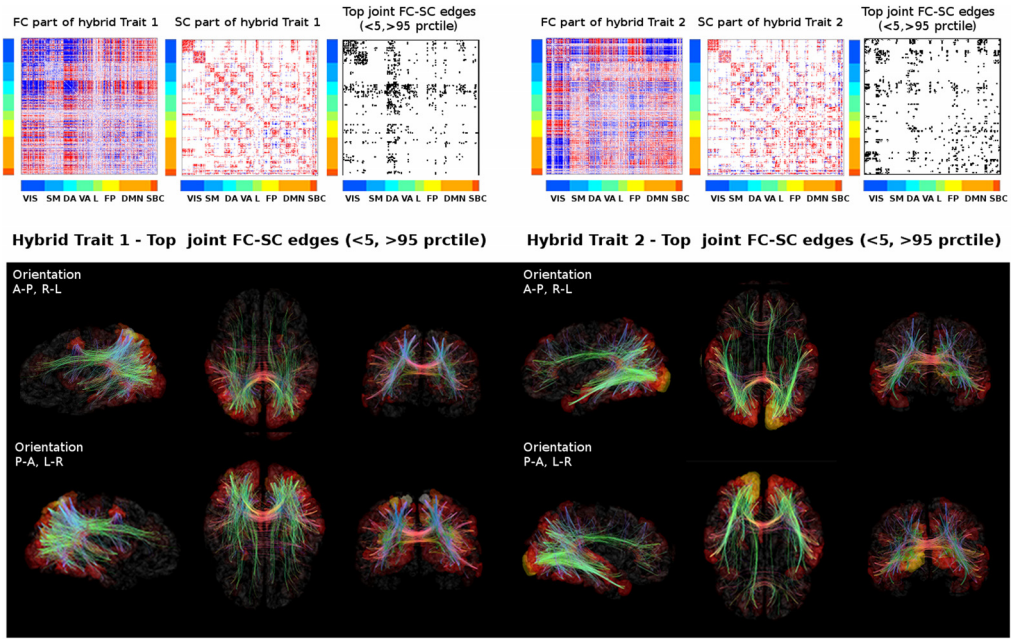


Figure 3. Visualizing task-sensitive joint functional-structural circuits in the human brain. Top: The hybrid traits (split in functional and structural patterns) shown in Figure 2 and the joint mask obtained from the product of the more extreme values (outside the [5 95] percentile range) in the corresponding FC and SC profiles. Bottom: The joint masks are projected onto brain renders, where tracts (color coded by direction; red: left-right; green: anterior-posterior; blue: superior-inferior) represent nonzero edges in the masks, and nodal strength (sum over columns of the masks) is mapped onto the cortical meshes, from low strength (black) to high nodal strength (bright yellow). The brain renders were obtained with MRtrix3 (Tournier et al., 2012).

Nodal strength:
In a weighted graph (i.e., where edges have assigned numerical values) node strength represents the total sum of the edge weights attached to the node.

DMN and FP regions (Figure 3). Notably, none of these task-switching circuits (i.e., the joint masks in Figure 3) were found when robust hybrid traits were obtained from the randomization of the SCs (see Materials and Methods for details and Figure S2). Indeed, it is noteworthy that the number of hybrid edges found in the joint FC-SC masks were significantly lower after randomization (see Figure S3).

The analysis of the nodal strength on the joint mask allows for an assessment of the overall centrality of each region on the hybrid task-sensitive traits (Figure 4). In the first hybrid trait, the main areas involved are the dorsal and ventral lobes, associated to attentional network connectivity, as expected. On the other hand, the left and right visual cortices dominate the nodal strength overview of the second hybrid trait (Figure 4).

DISCUSSION

The investigation of the interaction between structural and FC layers in large-scale human brain networks is one of the current challenges in brain connectomics (Falcon et al., 2016; Fornito et al., 2016; Honey et al., 2010; Mišić et al., 2016). The difficulty of addressing this problem is manifold: from the different data processing to the huge amount of information of difficult interpretation, to the necessity of estimating individual weights of group-level structural-functional circuits.

Here we proposed a framework, named hybrid connICA (which expands on connICA; Amico et al., 2017), that allows to extract, in a data-driven fashion, the most representative joint functional-structural (i.e., hybrid) patterns from a set of individual joint connectivity

Downloaded from http://www.mitpressjournals.org/doi/pdf/10.1162/netn_a_00049 by guest on 28 March 2024

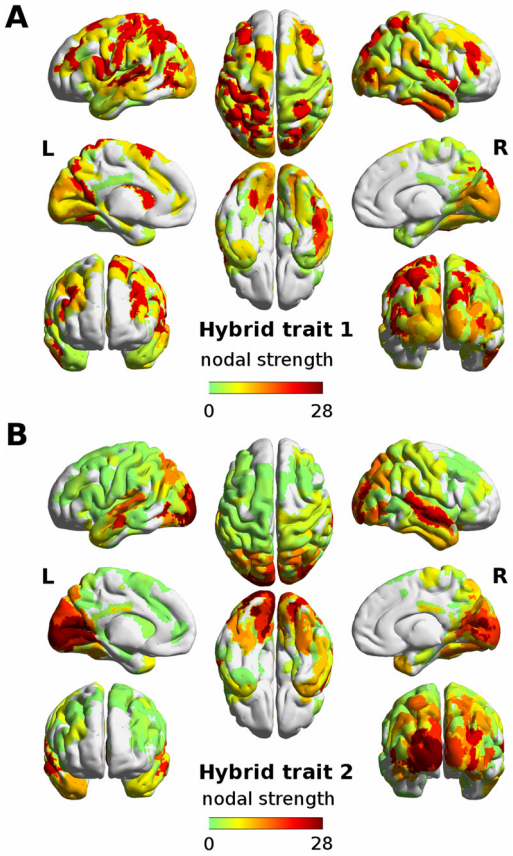


Figure 4. Node centrality of the hybrid task-sensitive traits. The strength per region computed as sum of nonzero values in the joint FC-SC mask, for the (A) first and (B) second hybrid trait. The mask was obtained by taking only the most extreme edges in the FC and SC parts of the two hybrid traits (outside the 5th and 95th percentile of each distribution of values). Note how the first trait mainly involves attentional-related areas in the dorsal and ventral lobes lobe, whereas both left and right visual cortices dominate in the second trait. The brain renders were obtained with BrainNet Viewer (Xia, Wang, & He, 2013).

profiles (see Figure 1). We tested this methodology on the HCP data benchmark to retrieve the hybrid connectivity subsystem related to changes in functional tasks and resting state (Figures 2 and 3).

The hybrid connICA extracted two main task-dependent traits; the first, encompassing the within- and between-network connections of dorsal attentional and visual areas, as well as subcortical structures (Figure 2). The second hybrid trait associated to task switching mainly specializes in the connectivity between the visual and frontoparietal, DMN, and subcortical networks (Figure 2). These findings are in line with previous research showing that these are the main areas (attentional cortices, DMN, visual, and subcortical regions) undergoing major changes when passing from rest to task sessions (Cole, Bassett, Power, Braver, & Petersen, 2014; Fox & Raichle, 2007; Hasson, Nusbaum, & Small, 2009; Hermundstad et al., 2013; Tavor et al., 2016). Recent studies also reported the existence of an "intrinsic functional architecture" (Cole et al., 2014) that shapes the brain's functional network architecture during task performance (Tavor et al., 2016). These findings suggest that a set of small but consistent changes in FC across tasks might distinguish task states from rest (Cole et al., 2014), and it might also allow us to predict task states from the intrinsic resting-state organization (Tavor et al., 2016). We also assessed the reproducibility of the results by evaluating the two most frequent hybrid traits

Downloaded from http://www.mitpressjournals.org/doi/pdf/10.1162/netn_a_00049 by guest on 28 March 2024

at a coarser grain resolution (Figure S5). Interestingly, a high resemblance from the perspective of an RSN (within and between) was found, suggesting that the method presented here shows consistency in the results across brain spatial scales and resolutions.

Here, we took one step forward in this direction by using a hybrid connICA approach to map the main joint FC-SC circuitry involved in task switching (Figure 3). Interestingly, the intrinsic resting-state organization of a human brain both at the functional and structural level was also recovered, even though it was not associated to changes across tasks. Indeed, one robust trait captured all the main functional and structural connections of RSN blocks (hybrid trait 3; Figure S4).

One benefit of this methodology resides in the possibility to extract and visualize "cities" (cortical functional nodes) and highways (structural connections) corresponding to specific subsystems simultaneously (Figure 3). In the case of this work, functional-structural patterns that change depending on whether the subject is at rest or performing a specific task (Figure 3). Notably, both hybrid traits capture two main aspects of brain network connectivity: integration (in the sense of functional interaction between networks) and segregation (expressed as main within-network connectivity between structural circuits; Figure 2 and Figure S4; Tononi, Sporns, & Edelman, 1994). It is worth stressing here that the resulting hybrid patterns are by all means entangled together. Notably, it is not likely to retrieve the same joint subsystems without the real connectivity structure (Figure S3). When the SCs were randomized (see Figure S3 and Materials and Methods), it was not possible to retrieve any of the hybrid joint pathways presented in Figure 3 (i.e., the number of nonzero values in the FC-SC mask significantly lowered after randomization; see Figure S3).

There are several advantages in applying a data-driven procedure such as hybrid connICA. The compression of the meaningful information into a few hybrid connectivity layers that are robust, independent, and task sensitive is one of the major points. In addition, the subject weights associated to each hybrid trait are unique, meaning that there are single individual weights that allow us to recover the structural-functional subsystem at the single-subject level (e.g., the ICA procedure was performed at once by concatenating structural and functional profiles, hence it provided unique sets of weights associated to the FC and SC connectomes). This might ease inferences at the individual level with cognitive, genetic variables directly on the weights, and avoid multiple comparisons when working with multidimensional matrices. Our approach based on independent group-level hybrid traits with associated individual weights adds to recently proposed data-driven methods, where group-level orthogonal covarying structural-functional patterns are extracted based on singular value decomposition (Mišić et al., 2016). Although these approaches are focused on the integration of different modalities, frameworks such as canonical correlation analysis (Irimia & Van Horn, 2013) allow us to disentangle which modalities are responsible for associations between different brain regions.

Here we showed an application of the hybrid connICA in disentangling task-dependent joint FC-SC circuits in healthy young adults. Next steps for using this framework will involve the investigation of hybrid patterns in clinical populations where heterogeneous individual structural damage is usually associated with a rich repertoire of different functional responses (such as in Parkinson's disease, Alzheimer's disease, traumatic brain injury, disorders of consciousness, etc.). This method can then provide a data-driven way to disentangle the main circuits associated with the disease (similarly to the functional connICA; Amico et al., 2017; Contreras et al., 2017), while assessing structural and functional changes at the same time. This might also allow researchers to investigate and make inferences on the structural and functional

Downloaded from http://www.mitpressjournals.org/doi/pdf/10.1162/netn_a_00049 by guest on 28 March 2024

circuitries involved by compressing them into a few hybrid traits. The flexibility of the method enables for extending the approach to layers other than the structural ones. For instance, one may substitute the SC layer proposed in this work with other network measures such as modularity, efficiency, or search information. Also, one may assess the multimodal integration of different functional modalities such as electroencephalography at different frequency bands, or magnetoencephalography, among others.

This study has several limitations. The optimal size of the cohort for the extraction of the hybrid connICA components needs to be further investigated. Similarly, the best choice of the starting number of ICA components (here set to 10; see Figure S1) and the threshold for the final selection of the most frequent components over multiple ICA runs (here set to 50%) depends on the research question at hand. It is important to have a priori hypotheses for filtering the robust traits for analyses. For instance, here we used intraclass correlation among tasks as a criterion. Also, in recent clinical studies, multilinear models were used to associate the connectivity traits to crucial behavioral and/or clinical variables (Amico et al., 2017; Contreras et al., 2017). Despite that a state-of-the-art tractography (SIFT2, MRtrix3) algorithm was used in this study, further exploration of the sensitivity and specificity of the hybrid traits to different tractography could be performed. Finally, for the ICA extraction to work properly, we also strongly recommend for the range of the two connectivity profiles concatenated to be consistent across edges. Here we proposed the use of SC-based correlations. However, different normalizations could be applied for making SC and FC magnitudes comparable or at least more homogeneous (e.g., using absolute values, dividing by the maximum value, or by applying L1 and L2 norms (Calhoun et al., 2006a; Kessler et al., 2014).

In conclusion, we here proposed a novel data-driven approach, hybrid connICA (successor of connICA; Amico et al., 2017), to disentangle the most influential functional-structural connectivity patterns related to changes in brain networks across tasks and resting state. Our results shed light on the key hybrid circuitry (both functional and structural) involved in the differentiation of connectivity profiles across different tasks. By simultaneously extracting structural-functional subsystems, the proposed methodology might improve our understanding of connectivity changes associated to brain pathologies.

AUTHOR CONTRIBUTIONS

Enrico Amico: Conceptualization; Data curation; Methodology; Writing – original draft; Writing – review & editing. Joaquín Goñi: Conceptualization; Data curation; Formal analysis; Funding acquisition; Investigation; Methodology; Supervision; Validation; Writing – original draft; Writing – review & editing.

FUNDING INFORMATION

Data were provided, in part, by the Human Connectome Project, WU-Minn Consortium (Principal Investigators: David Van Essen and Kamil Uğurbil; 1U54MH091657) funded by the 16 NIH Institutes and Centers that support the NIH Blueprint for Neuroscience Research; and by the McDonnell Center for Systems Neuroscience at Washington University. This work was partially supported by NIH Grants R01EB022574 and by NIH R01MH108467 and by the Indiana Clinical and Translational Sciences Institute (Grant UL1TR001108) from the National Institutes of Health, National Center for Advancing Translational Sciences, Clinical and Translational Sciences Award.

Downloaded from http://www.mitpressjournals.org/doi/pdf/10.1162/netn_a_00049 by guest on 28 March 2024

SUPPORTING INFORMATION

The code used for extract hybrid connICA traits from joint FC-SC data is available on the CONNplexity lab website (https://engineering.purdue.edu/ConnplexityLab).

REFERENCES

Amico, E., & Goñi, J. (2018). The quest for identifiability in human functional connectomes. *Scientific Report*. Accepted for publication.

Amico, E., & Goñi, J. (2018). Supplemental Material for "Mapping hybrid functional-structural connectivity traits in the human connectome." *Network Neuroscience*, *2*(3), 306–322. https://doi.org/10.1162/netn_a_00049

Amico, E., Marinazzo, D., Di Perri, C., Heine, L., Annen, J., Martial, C., . . . Goñi, J. (2017). Mapping the functional connectome traits of levels of consciousness. *NeuroImage*, *148*, 201–211. https://doi.org/10.1016/j.neuroimage.2017.01.020

Andersson, J. L. R., Skare, S., & Ashburner, J. (2003). How to correct susceptibility distortions in spin-echo echo-planar images: Application to diffusion tensor imaging. *NeuroImage*, *20*(2), 870–888. https://doi.org/10.1016/S1053-8119(03)00336-7

Barch, D. M., Burgess, G. C., Harms, M. P., Petersen, S. E., Schlaggar, B. L., Corbetta, M., . . . Van Essen, D. C. (2013). Function in the human connectome: Task-fMRI and individual differences in behavior. *NeuroImage*, *80*, 169–189. https://doi.org/10.1016/j.neuroimage.2013.05.033

Bartko, J. J. (1966). The intraclass correlation coefficient as a measure of reliability. *Psychological Reports*, *19*(1), 3–11. https://doi.org/10.2466/pr0.1966.19.1.3

Bullmore, E., & Sporns, O. (2009). Complex brain networks: Graph theoretical analysis of structural and functional systems. *Nature Reviews Neuroscience*, *10*(3), 186–198. https://doi.org/10.1038/nrn2575

Calhoun, V. D., Adali, T., Giuliani, N. R., Pekar, J. J., Kiehl, K. A., & Pearlson, G. D. (2006a). Method for multimodal analysis of independent source differences in schizophrenia: Combining gray matter structural and auditory oddball functional data. *Human Brain Mapping*, *27*(1), 47–62. https://doi.org/10.1002/hbm.20166

Calhoun, V. D., Adali, T., Kiehl, K. A., Astur, R., Pekar, J. J., & Pearlson, G. D. (2006b). A method for multitask fMRI data fusion applied to schizophrenia. *Human Brain Mapping*, *27*(7), 598–610. https://doi.org/10.1002/hbm.20204

Calhoun, V. D., Liu, J., & Adali, T. (2009). A review of group ICA for fMRI data and ICA for joint inference of imaging, genetic, and ERP data. *NeuroImage*, *45*(1), S163–S172. https://doi.org/10.1016/j.neuroimage.2008.10.057

Caruyer, E., Cheng, J., Lenglet, C., Sapiro, G., Jiang, T., & Deriche, R. (2011). Optimal Design of Multiple Q-shells experiments for Diffusion MRI. Presented at the MICCAI Workshop on Computational Diffusion MRI - CDMRI'11. Retrieved from https://hal.inria.fr/inria-00617663/document

Christiaens, D., Reisert, M., Dhollander, T., Sunaert, S., Suetens, P., & Maes, F. (2015). Global tractography of multi-shell diffusion-weighted imaging data using a multi-tissue model. *NeuroImage*, *123*, 89–101. https://doi.org/10.1016/j.neuroimage.2015.08.008

Cole, M. W., Bassett, D. S., Power, J. D., Braver, T. S., & Petersen, S. E. (2014). Intrinsic and task-evoked network architectures of the human brain. *Neuron*, *83*(1), 238–251. https://doi.org/10.1016/j.neuron.2014.05.014

CONNplexity Lab. (2018). Brain Connectomics & Complex networks. Retrieved from https://engineering.purdue.edu/ConnplexityLab

Contreras, J. A., Goñi, J., Risacher, S. L., Amico, E., Yoder, K., Dzemidzic, M., . . . Saykin, A. J. (2017). Cognitive complaints in older adults at risk for Alzheimer's disease are associated with altered resting-state networks. *Alzheimer's and Dementia: Diagnosis, Assessment, and Disease Monitoring*, *6*, 40–49. https://doi.org/10.1016/j.dadm.2016.12.004

Destrieux, C., Fischl, B., Dale, A., & Halgren, E. (2010). Automatic parcellation of human cortical gyri and sulci using standard anatomical nomenclature. *NeuroImage*, *53*(1), 1–15. https://doi.org/10.1016/j.neuroimage.2010.06.010

Falcon, M. I., Jirsa, V., & Solodkin, A. (2016). A new neuroinformatics approach to personalized medicine in neurology: The virtual brain. *Current Opinion in Neurology*, *29*(4), 429–436. https://doi.org/10.1097/WCO.0000000000000344

Finn, E. S., Shen, X., Scheinost, D., Rosenberg, M. D., Huang, J., Chun, M. M., . . . Constable, R. T. (2015). Functional connectome fingerprinting: Identifying individuals using patterns of brain connectivity. *Nature Neuroscience*, *18*(11), 1664–1671. https://doi.org/10.1038/nn.4135

Fischl, B., van der Kouwe, A., Destrieux, C., Halgren, E., Ségonne, F., Salat, D. H., . . . Dale, A. M. (2004). Automatically parcellating the human cerebral cortex. *Cerebral Cortex*, *14*(1), 11–22. https://doi.org/10.1093/cercor/bhg087

Fornito, A., Zalesky, A., & Breakspear, M. (2015). The connectomics of brain disorders. *Nature Reviews Neuroscience*, *16*(3), 159–172. https://doi.org/10.1038/nrn3901

Fornito, A., Zalesky, A., & Bullmore, E. (2016). *Fundamentals of Brain Network Analysis*. Amsterdam, the Netherlands: Academic Press.

Fox, M. D., & Raichle, M. E. (2007). Spontaneous fluctuations in brain activity observed with functional magnetic resonance imaging. *Nature Reviews Neuroscience*, *8*(9), 700–711. https://doi.org/10.1038/nrn2201

Friston, K. J. (2011). Functional and effective connectivity: A review. *Brain Connectivity*, *1*(1), 13–36. https://doi.org/10.1089/brain.2011.0008

Glasser, M. F., Coalson, T. S., Robinson, E. C., Hacker, C. D., Harwell, J., Yacoub, E., . . . Van Essen, D. C. (2016). A multi-modal

Downloaded from http://www.mitpressjournals.org/doi/pdf/10.1162/netn_a_00049 by guest on 28 March 2024

parcellation of human cerebral cortex. *Nature*, *536*(7615), 171–178. https://doi.org/10.1038/nature18933

Glasser, M. F., Sotiropoulos, S. N., Wilson, J. A., Coalson, T. S., Fischl, B., Andersson, J. L., . . . Jenkinson, M. (2013). The minimal preprocessing pipelines for the Human Connectome Project. *NeuroImage*, *80*, 105–124. https://doi.org/10.1016/j.neuroimage.2013.04.127

Goñi, J., Corominas-Murtra, B., Solé, R. V., & Rodríguez-Caso, C. (2010). Exploring the randomness of directed acyclic networks. *Physical Review E*, *82*(6), 066115. https://doi.org/10.1103/PhysRevE.82.066115

Goñi, J., Heuvel, M. P. van den, Avena-Koenigsberger, A., Mendizabal, N. V. de, Betzel, R. F., Griffa, A., . . . Sporns, O. (2014). Resting-brain functional connectivity predicted by analytic measures of network communication. *Proceedings of the National Academy of Sciences*, *111*(2), 833–838. https://doi.org/10.1073/pnas.1315529111

Hasson, U., Nusbaum, H. C., & Small, S. L. (2009). Task-dependent organization of brain regions active during rest. *Proceedings of the National Academy of Sciences*, *106*(26), 10841–10846. https://doi.org/10.1073/pnas.0903253106

Hermundstad, A. M., Bassett, D. S., Brown, K. S., Aminoff, E. M., Clewett, D., Freeman, S., . . . Carlson, J. M. (2013). Structural foundations of resting-state and task-based functional connectivity in the human brain. *Proceedings of the National Academy of Sciences*, *110*(15), 6169–6174. https://doi.org/10.1073/pnas.1219562110

Honey, C. J., Kötter, R., Breakspear, M., & Sporns, O. (2007). Network structure of cerebral cortex shapes functional connectivity on multiple time scales. *Proceedings of the National Academy of Sciences*, *104*(24), 10240–10245. https://doi.org/10.1073/pnas.0701519104

Honey, C. J., Sporns, O., Cammoun, L., Gigandet, X., Thiran, J. P., Meuli, R., & Hagmann, P. (2009). Predicting human resting-state functional connectivity from structural connectivity. *Proceedings of the National Academy of Sciences*, *106*(6), 2035–2040. https://doi.org/10.1073/pnas.0811168106

Honey, C. J., Thivierge, J.-P., & Sporns, O. (2010). Can structure predict function in the human brain? *NeuroImage*, *52*(3), 766–776. https://doi.org/10.1016/j.neuroimage.2010.01.071

Hyvarinen, A. (1999). Fast ICA for noisy data using Gaussian moments. In *Proceedings of the 1999 IEEE International Symposium on Circuits and Systems, 1999. ISCAS '99* (Vol. 5, pp. 57–61). https://doi.org/10.1109/ISCAS.1999.777510

Hyvärinen, A., & Oja, E. (2000). Independent component analysis: Algorithms and applications. *Neural Networks*, *13*(4), 411–430. https://doi.org/10.1016/S0893-6080(00)00026-5

Irimia, A., & Van Horn, J. D. (2013). The structural, connectomic and network covariance of the human brain. *NeuroImage*, *66*, 489–499. https://doi.org/10.1016/j.neuroimage.2012.10.066

Jenkinson, M., Beckmann, C. F., Behrens, T. E. J., Woolrich, M. W., & Smith, S. M. (2012). FSL. *NeuroImage*, *62*(2), 782–790. https://doi.org/10.1016/j.neuroimage.2011.09.015

Jeurissen, B., Tournier, J.-D., Dhollander, T., Connelly, A., & Sijbers, J. (2014). Multi-tissue constrained spherical deconvolution for improved analysis of multi-shell diffusion MRI data. *NeuroImage*, *103*, 411–426. https://doi.org/10.1016/j.neuroimage.2014.07.061

Jolliffe, I. (2014). Principal component analysis. In *Wiley Statsref: Statistics Reference Online*. John Wiley & Sons. https://doi.org/10.1002/9781118445112.stat06472

Kessler, D., Angstadt, M., & Sripada, C. (2016). Growth charting of brain connectivity networks and the identification of attention impairment in youth. *JAMA Psychiatry*, *73*(5), 481–489. https://doi.org/10.1001/jamapsychiatry.2016.0088

Kessler, D., Angstadt, M., Welsh, R. C., & Sripada, C. (2014). Modality-spanning deficits in attention-deficit/hyperactivity disorder in functional networks, gray matter, and white matter. *Journal of Neuroscience*, *34*(50), 16555–16566. https://doi.org/10.1523/JNEUROSCI.3156-14.2014

Marcus, D., Harwell, J., Olsen, T., Hodge, M., Glasser, M., Prior, F., . . . Van Essen, D. (2011). Informatics and data mining tools and strategies for the Human Connectome Project. *Frontiers in Neuroinformatics*, *5*. https://doi.org/10.3389/fninf.2011.00004

McGraw, K. O., & Wong, S. P. (1996). Forming inferences about some intraclass correlation coefficients. *Psychological Methods*, *1*(1), 30–46. https://doi.org/10.1037/1082-989X.1.1.30

Mišić, B., Betzel, R. F., Reus, D., A, M., Heuvel, V. D., P, M., . . . Sporns, O. (2016). Network-level structure-function relationships in human neocortex. *Cerebral Cortex*, *26*(7), 3285–3296. https://doi.org/10.1093/cercor/bhw089

Power, J. D., Mitra, A., Laumann, T. O., Snyder, A. Z., Schlaggar, B. L., & Petersen, S. E. (2014). Methods to detect, characterize, and remove motion artifact in resting state fMRI. *NeuroImage*, *84*, 320–341. https://doi.org/10.1016/j.neuroimage.2013.08.048

Rubinov, M., & Sporns, O. (2010). Complex network measures of brain connectivity: Uses and interpretations. *NeuroImage*, *52*(3), 1059–1069. https://doi.org/10.1016/j.neuroimage.2009.10.003

Salimi-Khorshidi, G., Douaud, G., Beckmann, C. F., Glasser, M. F., Griffanti, L., & Smith, S. M. (2014). Automatic denoising of functional MRI data: Combining independent component analysis and hierarchical fusion of classifiers. *NeuroImage*, *90*, 449–468. https://doi.org/10.1016/j.neuroimage.2013.11.046

Särelä, J., & Vigário, R. (2003). Overlearning in marginal distribution-based ICA: Analysis and solutions. *Journal of Machine Learning Research*, *4*(Dec), 1447–1469.

Shen, X., Finn, E. S., Scheinost, D., Rosenberg, M. D., Chun, M. M., Papademetris, X., & Constable, R. T. (2017). Using connectome-based predictive modeling to predict individual behavior from brain connectivity. *Nature Protocols*, *12*(3), 506–518. https://doi.org/10.1038/nprot.2016.178

Shrout, P. E., & Fleiss, J. L. (1979). Intraclass correlations: Uses in assessing rater reliability. *Psychological Bulletin*, *86*(2), 420–428. https://doi.org/10.1037/0033-2909.86.2.420

Smith, R. E., Tournier, J.-D., Calamante, F., & Connelly, A. (2012). Anatomically-constrained tractography: Improved diffusion MRI streamlines tractography through effective use of anatomical information. *NeuroImage*, *62*(3), 1924–1938. https://doi.org/10.1016/j.neuroimage.2012.06.005

Smith, R. E., Tournier, J.-D., Calamante, F., & Connelly, A. (2013). SIFT: spherical-deconvolution informed filtering of tractograms. *NeuroImage*, *67*, 298–312. https://doi.org/10.1016/j.neuroimage.2012.11.049

Downloaded from http://www.mitpressjournals.org/doi/pdf/10.1162/netn_a_00049 by guest on 28 March 2024

Smith, R. E., Tournier, J.-D., Calamante, F., & Connelly, A. (2015). SIFT2: Enabling dense quantitative assessment of brain white matter connectivity using streamlines tractography. *NeuroImage*, *119*, 338–351. https://doi.org/10.1016/j.neuroimage.2015.06.092

Smith, S. M., Beckmann, C. F., Andersson, J., Auerbach, E. J., Bijsterbosch, J., Douaud, G., . . . Glasser, M. F. (2013). Resting-state fMRI in the Human Connectome Project. *NeuroImage*, *80*, 144–168. https://doi.org/10.1016/j.neuroimage.2013.05.039

Sotiropoulos, S. N., Jbabdi, S., Xu, J., Andersson, J. L., Moeller, S., Auerbach, E. J., . . . Behrens, T. E. J. (2013). Advances in diffusion MRI acquisition and processing in the Human Connectome Project. *NeuroImage*, *80*, 125–143. https://doi.org/10.1016/j.neuroimage.2013.05.057

Sporns, O. (2011). The human connectome: a complex network. *Annals of the New York Academy of Sciences*, *1224*(1), 109–125. https://doi.org/10.1111/j.1749-6632.2010.05888.x

Stejskal, E. O., & Tanner, J. E. (1965). Spin diffusion measurements: Spin echoes in the presence of a time-dependent field gradient. *The Journal of Chemical Physics*, *42*(1), 288–292. https://doi.org/10.1063/1.1695690

Tavor, I., Jones, O. P., Mars, R. B., Smith, S. M., Behrens, T. E., & Jbabdi, S. (2016). Task-free MRI predicts individual differences in brain activity during task performance. *Science*, *352*(6282), 216–220. https://doi.org/10.1126/science.aad8127

Tononi, G., Sporns, O., & Edelman, G. M. (1994). A measure for brain complexity: relating functional segregation and integration in the nervous system. *Proceedings of the National Academy of Sciences*, *91*(11), 5033–5037.

Tournier, J.-D., Calamante, F., & Connelly, A. (2012). MRtrix: Diffusion tractography in crossing fiber regions. *International Journal of Imaging Systems and Technology*, *22*(1), 53–66. https://doi.org/10.1002/ima.22005

Uğurbil, K., Xu, J., Auerbach, E. J., Moeller, S., Vu, A. T., Duarte-Carvajalino, J. M., . . . Yacoub, E. (2013). Pushing spatial and temporal resolution for functional and diffusion MRI in the Human Connectome Project. *NeuroImage*, *80*, 80–104. https://doi.org/10.1016/j.neuroimage.2013.05.012

Van Essen, D. C., Smith, S. M., Barch, D. M., Behrens, T. E. J., Yacoub, E., & Ugurbil, K. (2013). The WU-Minn Human Connectome Project: An overview. *NeuroImage*, *80*, 62–79. https://doi.org/10.1016/j.neuroimage.2013.05.041

Van Essen, D. C., Ugurbil, K., Auerbach, E., Barch, D., Behrens, T. E. J., Bucholz, R., . . . WU-Minn HCP Consortium. (2012). The Human Connectome Project: A data acquisition perspective. *NeuroImage*, *62*(4), 2222–2231. https://doi.org/10.1016/j.neuroimage.2012.02.018

Xia, M., Wang, J., & He, Y. (2013). BrainNet Viewer: A network visualization tool for human brain connectomics. *PloS one*, *8*(7), e68910. https://doi.org/10.1371/journal.pone.0068910

Yeo, B. T. T., Krienen, F. M., Sepulcre, J., Sabuncu, M. R., Lashkari, D., Hollinshead, M., . . . Buckner, R. L. (2011). The organization of the human cerebral cortex estimated by intrinsic functional connectivity. *Journal of Neurophysiology*, *106*(3), 1125–1165. https://doi.org/10.1152/jn.00338.2011

Downloaded from http://www.mitpressjournals.org/doi/pdf/10.1162/netn_a_00049 by guest on 28 March 2024